

# Exploring the Catalytic Potential of ZIF-90: Solventless and Co-Catalyst-Free Synthesis of Propylene Carbonate from Propylene Oxide and CO<sub>2</sub>

Jose Tharun,<sup>[a]</sup> George Mathai,<sup>[b]</sup> Amal Cherian Kathalikkattil,<sup>[a]</sup> Roshith Roshan,<sup>[a]</sup> Yong-Sun Won,<sup>[c]</sup> Sung June Cho,<sup>[d]</sup> Jong-San Chang,<sup>[e]</sup> and Dae-Won Park<sup>\*[a]</sup>

Herein we report the application of ZIF-90, which is a highly porous zeolitic imidazolate framework, as a novel catalyst for the cycloaddition of propylene oxide (PO) with CO<sub>2</sub> in the absence of co-catalysts and solvents under moderate reaction conditions. The effects of various reaction parameters were investigated. The activity of ZIF-90 was compared with that of various metal-organic-framework (MOF)-based catalysts for the

cycloaddition of PO with CO<sub>2</sub>. Density functional theory calculations elucidated the role of ZIF-90 in creating a favorable environment for the PO-CO<sub>2</sub> cycloaddition reaction. A reaction mechanism for the ZIF-90-catalyzed PO-CO<sub>2</sub> cycloaddition on the basis of DFT calculations is proposed and the regeneration of ZIF-90 is discussed.

## Introduction

Zeolitic imidazolate frameworks (ZIFs) are an emerging class of metal-organic frameworks (MOFs) with three-dimensional structures connected by metal centers and organic imidazolate linkers. The M-Im-M binding angle in these MOFs, in which M is Zn or Co and Im is imidazolate, is equivalent to the Si-O-Si preferred angle (145 °C) in zeolites, which is why they are referred to as ZIFs.<sup>[1]</sup> ZIFs are known for their remarkably high chemical and thermal stabilities relative to those of MOFs reported to date and their permanent porosity, which makes them ideal for gas adsorption.<sup>[2]</sup> Removal of atmospheric CO<sub>2</sub> and its subsequent transformation into valuable products is an optimal solution to the major global concern of mitigating global warming and resource utilization.<sup>[3]</sup> Cycloaddition of CO<sub>2</sub> with epoxides to produce five-membered cyclic carbonates is an atom-economic route to CO<sub>2</sub> fixation. Cyclic carbonates can be applied as aprotic polar solvents for degreasing, paint-strip-

ping, and cleaning processes; they are also useful intermediates for the synthesis of polycarbonates, electrolytes in lithium-ion batteries, and green solvents.<sup>[4]</sup> Various catalysts have been developed for this reaction, including those based on alkali metal halides, metal oxides, titano silicates, metal complexes, and diverse homogeneous and heterogeneous ionic liquids (ILs).<sup>[5]</sup>

The catalytic application of MOFs towards the cycloaddition of CO<sub>2</sub> and epoxides is an expanding area of interest; accordingly, several studies have been reported.<sup>[6]</sup> However, most of the MOF-based CO<sub>2</sub>-epoxide cycloaddition reactions employ either co-catalysts or solvents; without these additives, the catalytic performance is relatively poor.<sup>[6a-i]</sup> Hence, we focused on implementing new MOFs that can activate the cycloaddition reaction without additional components. This led us to ZIFs, which comprise a new class of MOFs with great potential for gas adsorption and storage, molecular separation, catalysis, drug delivery, and molecular sensing because of their large internal surface area and uniform pore structures.<sup>[7]</sup> Thus, the ZIF-90 crystal, which has larger pores and greater surface area, is applied as a catalyst for the cycloaddition of propylene oxide (PO) with CO<sub>2</sub> in this study (Scheme 1). Despite the recent plethora of reported MOFs for CO<sub>2</sub> fixation in chemical transformations, none of the reports have included theoretical validation of the process. Hence, we performed density func-

[a] Dr. J. Tharun, Dr. A. C. Kathalikkattil, Dr. R. Roshan, Prof. D.-W. Park  
Division of Chemical and Biomolecular Engineering  
Pusan National University  
Busan 609-735 (Korea)  
Fax: (+82)51-512-8563  
E-mail: dwpark@pusan.ac.kr

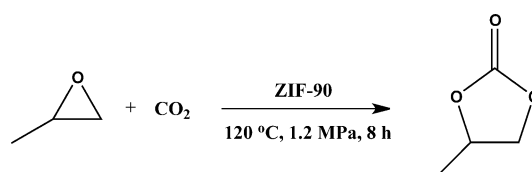
[b] Dr. G. Mathai  
Sacred Heart College  
Thevara, Kochi 682-013 (India)

[c] Prof. Y.-S. Won  
Pukyung National University  
Busan (Korea)

[d] Prof. S. J. Cho  
Chonnam National University  
Gwangju (Korea)

[e] Prof. J.-S. Chang  
Korea Research Institute of Chemical Technology  
Daejeon (Korea)

Supporting information for this article is available on the WWW under <http://dx.doi.org/10.1002/cplu.201402395>.



Scheme 1. Cycloaddition of PO and CO<sub>2</sub>.

tional theory (DFT) calculations, which are expected to elucidate the promising environment created by ZIF-90 in catalyzing the PO-CO<sub>2</sub> cycloaddition.

## Experimental Section

### Synthesis of ZIF-90

To synthesize ZIF-90 crystals,<sup>[7g,h]</sup> zinc(II) nitrate hexahydrate (1.488 g; Sigma Aldrich, 98%) and imidazole-2-carboxaldehyde (ICA; 1.921 g; Alfa Aesar, 97%) were dissolved in dimethyl formamide (DMF; 100 mL; TCI, 99.5%). The solution was heated at 100 °C for 18 h and then cooled to room temperature. The resultant light-orange crystalline material was separated from the solution by decantation. The crystals were washed with methanol and then dried at 60 °C for 12 h.

### Characterization

The surface of the ZIF-90 crystals was observed with an S-4200 field-emission scanning electron microscope (Hitachi). X-ray diffraction (XRD) patterns were obtained with a Philips PANalytical X'pert PRO power diffractometer operating at 40 kV and 30 mA by using Ni-filtered Cu<sub>Kα</sub> radiation ( $\lambda = 1.5404 \text{ \AA}$ ). The diffractograms were recorded in the  $2\theta$  range of 5–50°. FTIR spectra were obtained with an Avatar 370 Thermo Nicolet spectrophotometer at a resolution of 4 cm<sup>-1</sup>. CO<sub>2</sub> and NH<sub>3</sub> TPD profiles were acquired with a chemisorption analyzer (BEL-CAT) as follows. Prior to measurements, 0.1 g of the sample was activated in He (30 mL min<sup>-1</sup>) at 280 °C for 1 h. The sample was subsequently exposed to the pulses of CO<sub>2</sub> (10%) or NH<sub>3</sub> (10%) in He at 40 °C for 1 h. The sample was then flushed with He (30 mL min<sup>-1</sup>) for 1 h. TPD measurements were carried out by raising the temperature from 40 to 280 °C at a heating rate of 5 °C min<sup>-1</sup>. The textural properties of the ZIF-90 crystals were analyzed by recording an N<sub>2</sub> adsorption isotherm at 77 K with a BET apparatus (Microneritics ASAP 2020). The specific surface area was determined using the BET model equation. Thermogravimetric analysis (TGA) was conducted using ZIF-90 (3.656 mg) with an AutoTGA 2950 apparatus under a nitrogen flow of 100 mL min<sup>-1</sup> while heating from room temperature to 600 °C at a rate of 10 °C min<sup>-1</sup>.

### Theoretical methods

A structural illustration of ZIF-90 was produced based on the crystallographic information file (CIF) obtained from the database at <http://www.ccdc.cam.ac.uk/CCDC> no. 693596, as reported by Yaghi et al.<sup>[7h]</sup> The details of the sodalite topology and features of the cages as well as the orientations of the aldehyde groups of ZIF-90 were constructed and assessed using Mercury 3.3 and a demonstration version of Diamond Crystal and Molecular Structure Visualization software. Both PM3 and DFT calculations were performed using Gaussian 09 software for Microsoft Windows.<sup>[10]</sup> The four-membered ring (tetramer) structures were originally obtained by optimizing the relative arrangement of the ICAs by using PM3 calculations. The structures obtained by PM3 calculations were again optimized using DFT at the B3LYP/6-31G(d,p) level.

### Cycloaddition of PO with CO<sub>2</sub>

Synthesis of the cyclic carbonate from PO and CO<sub>2</sub> using ZIF-90 crystals (Scheme 1) was performed in a 50 mL stainless-steel auto-

clave equipped with a magnetic stirrer. For each typical batch operation, PO (42.9 mmol) and ZIF-90 crystals were introduced to the reactor without solvent. The reactor was then purged several times with CO<sub>2</sub> and pressurized with CO<sub>2</sub> to a preset pressure of 0.7–1.2 MPa at room temperature. Next, the reactor was heated to the desired temperature, and the reaction was initiated by stirring the reaction mixture at 600 rpm. After the reaction time had elapsed, cycloaddition was stopped by cooling the reaction mixture to 0 °C and the products were identified with a gas chromatograph (Agilent HP 6890 A) equipped with a capillary column (HP-5, 30 m × 0.25 μm) using a flame ionization detector. The product yield was determined using an internal standard method with biphenyl (0.05 g) as the standard.

## Results and Discussion

### Characterization

Synthesized ZIF-90 crystals were characterized using Brunauer–Emmett–Teller methods (Figure S1, Table S1) and thermogravimetric analysis (TGA; Figure S2) as presented in the Supporting Information. Figure 1 shows scanning electron microscopy (SEM) images of ZIF-90, which reveals the well-defined surface morphology. X-ray diffraction (XRD) patterns of the ZIF-90 crystal are shown in Figure 2. The Fourier-transform infrared (FTIR) spectroscopy of ZIF-90 is shown in Figure 3. A strong band around 1680 cm<sup>-1</sup> (C=O) provided evidence for the presence of aldehyde groups in ZIF-90 crystals. CO<sub>2</sub> and NH<sub>3</sub> temperature-programmed-desorption (TPD) profiles are also presented

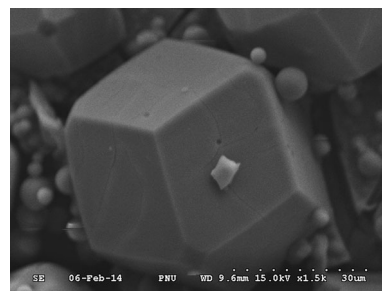


Figure 1. SEM image of ZIF-90.

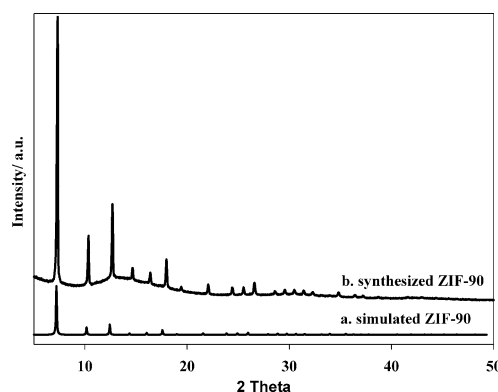


Figure 2. XRD pattern of ZIF-90: (a) simulated;<sup>[7h]</sup> (b) synthesized.

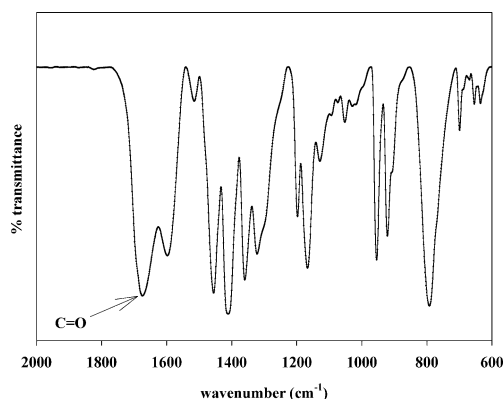


Figure 3. FTIR spectra of ZIF-90.

(Figures 4 and 5). From Table 1 (TPD), the presence of acidic and basic sites in ZIF-90 is demonstrated.

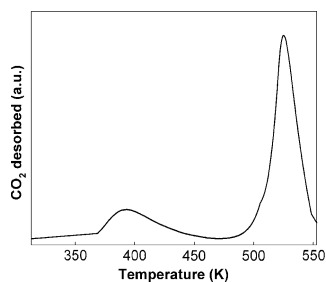


Figure 4. Temperature-programmed desorption of CO<sub>2</sub> from ZIF-90.

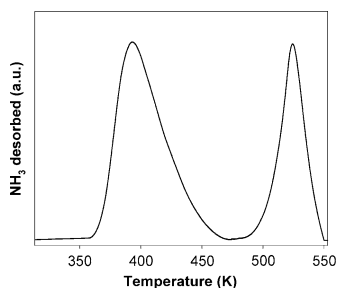


Figure 5. Temperature-programmed desorption of NH<sub>3</sub> from ZIF-90.

**Table 1.** The amount of acidic and basic sites in ZIF-90 according to CO<sub>2</sub> and NH<sub>3</sub> TPD experiments.

Catalyst	CO <sub>2</sub> TPD [mmol g <sup>-1</sup> ]			NH <sub>3</sub> TPD [mmol g <sup>-1</sup> ]		
	weak base <sup>[a]</sup>	strong base <sup>[b]</sup>	total	weak acid <sup>[c]</sup>	strong acid <sup>[d]</sup>	total
ZIF-90	3.14	1.91	5.05	10.06	34.43	44.49

[a] T = 351–470 K. [b] T = 470–553 K. [c] T = 358–474 K. [d] T = 474–551 K.

## Catalytic activity of ZIF-90

The catalytic activity of ZIF-90 towards the reaction of PO with CO<sub>2</sub> to produce propylene carbonate (PC) was investigated; the results are summarized in Table 2. No product formed in

**Table 2.** Effect of reaction parameters in the cycloaddition of PO and CO<sub>2</sub>.<sup>[a]</sup>

Entry	Catalyst amount [mg]	t [h]	T [°C]	P <sub>CO<sub>2</sub></sub> [MPa]	Conv. [%] <sup>[b]</sup>	Yield [%] <sup>[b]</sup>
1	–	8	120	1.2	0	0
2	10	8	120	1.2	16	14
3	20	8	120	1.2	45	39
4	30	8	120	1.2	88	81
5	50	8	120	1.2	89	81
6	30	2	120	1.2	13	11
7	30	4	120	1.2	32	27
8	30	10	120	1.2	90	83
9	30	8	90	1.2	13	11
10	30	8	100	1.2	21	18
11	30	8	140	1.2	89	82
12	30	8	120	0.7	38	34
13	30	8	120	1	63	56
14	30	8	120	2	90	83

[a] Reaction conditions: PO = 42.8 mmol, catalyst = ZIF-90. [b] Determined by GC.

the absence of a catalyst (Table 2, entry 1). In entries 2 to 5, the amount of ZIF-90 was varied with controlled reaction conditions of 120 °C, 1.2 MPa CO<sub>2</sub>, and a duration of eight hours. The best result of 88% conversion was obtained with 30 mg of catalyst (Table 2, entry 4); a further increase in the amount of catalyst to 50 mg (Table 2, entry 5) did not significantly increase the conversion. This could be attributed to the difficulty in dispersing the additional catalyst in the reaction mixture, which would eventually limit the mass transfer between the active sites and reactants.<sup>[5]</sup> Entries 4, 6, 7, and 8 of Table 2 show the effect of the reaction duration on the ZIF-90-catalyzed cycloaddition of PO with CO<sub>2</sub>: PO conversion increased with increasing time and reached a maximum of 88% at eight hours (Table 2, entry 4), and thereafter no significant increase in conversion was observed.

The effect of the reaction temperature on ZIF-90-catalyzed PO–CO<sub>2</sub> cycloaddition was also determined (Table 2, entries 4 and 9–11). The conversion of PO increased with temperature (88% at 120 °C); however, higher temperatures did not increase the conversion significantly. Similarly, the effect of CO<sub>2</sub> pressure was investigated (Table 2, entries 4 and 12–14): 1.2 MPa CO<sub>2</sub> (Table 2, entry 4) resulted in the highest conversion. A further increase in CO<sub>2</sub> pressure did not significantly increase conversion; this might be due to either inhibition of the interactions between propylene oxide and the catalyst by an excess amount of CO<sub>2</sub> pressure or lower PO concentration.<sup>[5g]</sup> Overall, the optimal reaction conditions for the ZIF-90-catalyzed PO–CO<sub>2</sub> cycloaddition were 30 mg of ZIF-90 at 120 °C and 1.2 MPa CO<sub>2</sub> for a duration of eight hours, which resulted

**Table 3.** Comparison of ZIF-90 with other MOF-based catalysts for the cycloaddition of PO and CO<sub>2</sub>.

Entry	PO [mmol]	MOF	Catalyst amount [mmol]	T [°C]	P <sub>CO<sub>2</sub></sub> [MPa]	t [h]	Co-catalyst [mmol]	Yield [%]	Ref.
1	18	Cr-MIL-101	0.22 (Cr)	25	0.8	24	TBABr (0.31)	82	[6f]
2	18	Fe-MIL-101	0.22 (Fe)	25	0.8	24	TBABr (0.31)	95	[6h]
3	18	HKUST-1	0.22 (Cu)	25	0.8	24	TBABr (0.31)	3	[6h]
4	20	MOF-5	0.52 (Zn)	50	6	4	–	0.1	[6t]
5	20	MOF-5	0.52 (Zn)	50	6	4	TBABr (0.5)	97.6	[6t]
6	285	MIXMOF	0.127	140	(615 mmol)	3	NEt <sub>4</sub> Br (0.1)	63	[6o]
7	10	Ni(salphen)-MOF	0.056 (Ni)	80	2	4	–	0	[6p]
8	10	Ni(salphen)-MOF	0.056 (Ni)	80	2	4	TBABr (0.3)	80	[6p]
9	18.6	CHB(M)	0.3	120	1.2	6	–	62	[6b]
10	500	IRMOF-3	0.52 (Zn)	140	2	5	–	2	[6m]
11	500	IRMOF-3	0.52 (Zn)	140	2	5	CH <sub>3</sub> I (0.5)	40	[6m]
12	18.6	ZIF-90	0.11 (Zn)	120	1.2	8	–	81	present work
13	200	–	–	125	2	1	TBABr (3.2)	73.1	[8]

in a good conversion of 88% and selectivity of 92%. The main byproduct of PO–CO<sub>2</sub> cycloaddition was propylene glycol.

A comparison of the catalytic performances of various MOFs for PO–CO<sub>2</sub> cycloaddition is shown in Table 3. For clarity, only MOFs that were directly applied (i.e., without any functionalization) or with a co-catalyst for PO–CO<sub>2</sub> cycloaddition were chosen. From all the entries except 9 and 12 of Table 3, it is evident that the MOFs applied to date for PO–CO<sub>2</sub> cycloaddition afforded only negligible activity in the absence of co-catalysts. Generally, quaternary ammonium salts, such as tetrabutylammonium bromide (TBABr), are employed as co-catalyst for MOF-catalyzed PO–CO<sub>2</sub> cycloaddition. Although TBABr alone reasonably catalyzes the reaction (Table 3, entry 13), MOFs alone did not appreciably catalyze PO–CO<sub>2</sub> cycloaddition. This result highlights the importance of developing MOFs that act as stand-alone catalysts with high activity for epoxide–CO<sub>2</sub> cycloaddition reactions. From Table 3, it is clear that CHB(M) (entry 9) and ZIF-90 (present work) are the only MOFs that show considerable activity in the absence of co-catalysts. Considering the reaction conditions and catalyst amounts shown in Table 3, ZIF-90 is an efficient MOF-based catalyst in the absence of co-catalysts and solvents. Also, the activity of ZIF-90 catalyst has been compared with traditional catalysts for the cycloaddition of PO and CO<sub>2</sub>; it is presented in the Supporting Information (Table S2).

### DFT studies

To understand the possibility of encapsulating PO and CO<sub>2</sub> in ZIF-90, which thereby leads to the activation of the cycloaddition reaction, DFT calculations were performed. Structurally, ZIF-90 has tetrahedral zinc atoms bridged by imidazole-2-carboxaldehyde (ICA) moieties through the imidazolate nitrogen atoms (Figure 6). Because ZIF-90 has a sodalite topology, it contains two types of cavities: (1) Four-membered ring cavities, that is, a tetramer that contains four Zn atoms and eight ICAs, and (2) six-membered ring cavities, that is, a hexamer that consists of six Zn atoms and twelve ICAs (Figure S3 in the Supporting Information).<sup>[7h]</sup> Both cavities are possible reaction sites for

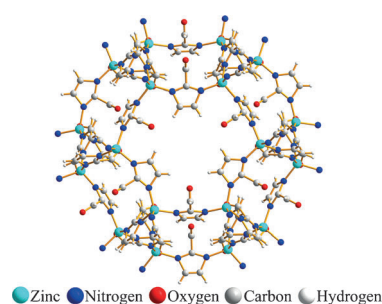


**Figure 6.** Ball-and-stick diagram depicting the Zn–Im–Zn linkages forming the sodalite cages (CIF file).<sup>[7h]</sup>

the cycloaddition of CO<sub>2</sub> with PO. Hence, various possible conformations of the tetramer were optimized using semiempirical PM3 calculations, and the structures were reoptimized using the B3LYP/6-31G(d,p) method. The results of the calculations show that in the lowest-energy conformation of the tetramer, the ICAs—that is, both those in the ring and the pendant ones—are oriented such that the CHO groups are alternately up and down (Figure 7). Further, the arrangements of the CHO groups minimize repulsion between the carbonyl oxygen atoms of adjacent ICAs. In the lowest-energy conformation, the Zn atoms occupy the corners of a square with a distance of 5.89 Å between two adjacent Zn atoms. Accordingly, the

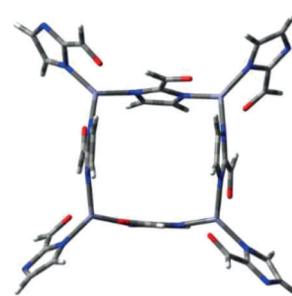


**Figure 7.** Lowest-energy conformation of ZIF-90 as a tetramer.

four-membered ring cavity has 5.89 Å edges. The Zn–N distances in the calculated structures vary from 2.019 to 2.022 Å in the ring and 1.974 Å for the pendent ICAs; these values are similar to those obtained by means of X-ray diffraction. Optimization of the possible reactant complex in which CO<sub>2</sub> and PO are encapsulated in the four-membered ring cavity was not successful owing to the small size of the cavity.

The lowest-energy structure of the six-membered ring (hexamer) in which the ICAs are alternately oriented up and down was optimized by using a semiempirical (PM3) method. The structure was reoptimized using DFT at the B3LYP/6-31G(d,p) level, as shown in Figure 8. The Zn–N distances in the calculat-

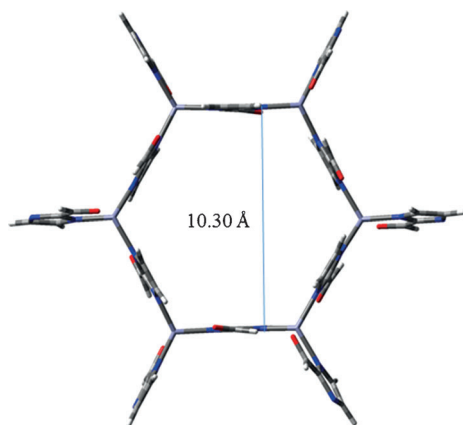


Figure 8. Lowest-energy conformation of ZIF-90 as a hexamer.

ed structure of the hexamer are 2.016 Å in the ring and 1.984 Å in the pendant ICAs; these values are also similar to those obtained using X-ray diffraction. The distance between two Zn atoms at alternate corners of the hexagon is 10.30 Å, thus indicating that the cavity formed by the hexamer is large enough to accommodate PO. As shown in the DFT structures and other reports,<sup>[1,2a,7h]</sup> ZIF-90, which is highly porous and has a large surface area, easily encapsulates small molecules such as PO and CO<sub>2</sub> in its large cage, which results in increased catalyst–substrate interactions and thus, higher activity.

### Reaction mechanism and reusability

For simplicity, a single repeating unit of ZIF-90 was chosen to explain the mechanism of the PO–CO<sub>2</sub> cycloaddition reaction through DFT. On the basis of DFT calculations, the activation energy required for the noncatalyzed cycloaddition of PO with CO<sub>2</sub> to produce PC was found to be 55–59 kcal mol<sup>−1</sup>, which is high for the reaction to proceed spontaneously and demands the use of a catalyst. Initially, the total energy of the reactant complex (PO, CO<sub>2</sub>, and ZIF-90) was preset to zero; the optimized geometrical arrangement of the reactant complex is shown in Scheme 2. An intermediate (Int-1) (−16.7 kcal mol<sup>−1</sup>) originated from the reactant complex. The O atom of PO was at a distance of 2.12 Å from the Zn of ZIF-90, whereas the O atom of the aldehyde group of ZIF-90 was at a distance of 2.81 Å from the C atom of CO<sub>2</sub>. The transition from Int-1 to

transition state (TS-1) resulted in the interaction of Zn atom of ZIF-90 with the O atom of PO (Zn–O = 1.94 Å), thereby leading to ring opening at the β carbon (βC) of the PO. The distance between the ring-opened βC and O was found to be 1.76 Å. In the next step, TS-1 dropped to a more stable Int-2 (−39.9 kcal mol<sup>−1</sup>), as a result of which the ring-opened βC<sub>(PO)</sub> and O<sub>(PO)</sub> distances became weaker (2.25 Å) and the Zn–O interaction between ZIF-90 and PO became stronger (1.86 Å). The transition from Int-2 to TS-2 produced the following events: (a) The ring-opened βC<sub>(PO)</sub> and O<sub>(PO)</sub> distance became even longer (2.43 Å); (b) the Zn–O interaction became stronger (1.78 Å); and (c) the C atom of CO<sub>2</sub> moved closer to the O atom of the aldehyde group of ZIF-90 (i.e., from 2.78 to 1.72 Å), whereby the geometry of the CO<sub>2</sub> molecule transformed from a linear to a bent structure. Then TS-2 dropped to intermediate Int-3 (−23.6 kcal mol<sup>−1</sup>), whereby the CO<sub>2</sub> molecule became tethered between PO and ZIF-90 to create an eight-membered stable cyclic intermediate ring. In TS-3, the eight-membered intermediate was ruptured by the interaction of the O<sub>CO<sub>2</sub></sub> atom in the eight-membered ring with the Zn of ZIF-90. Cycloaddition occurred in the next step to form another stable intermediate (Int-4; −26.1 kcal mol<sup>−1</sup>), which ultimately rendered the desired PC.

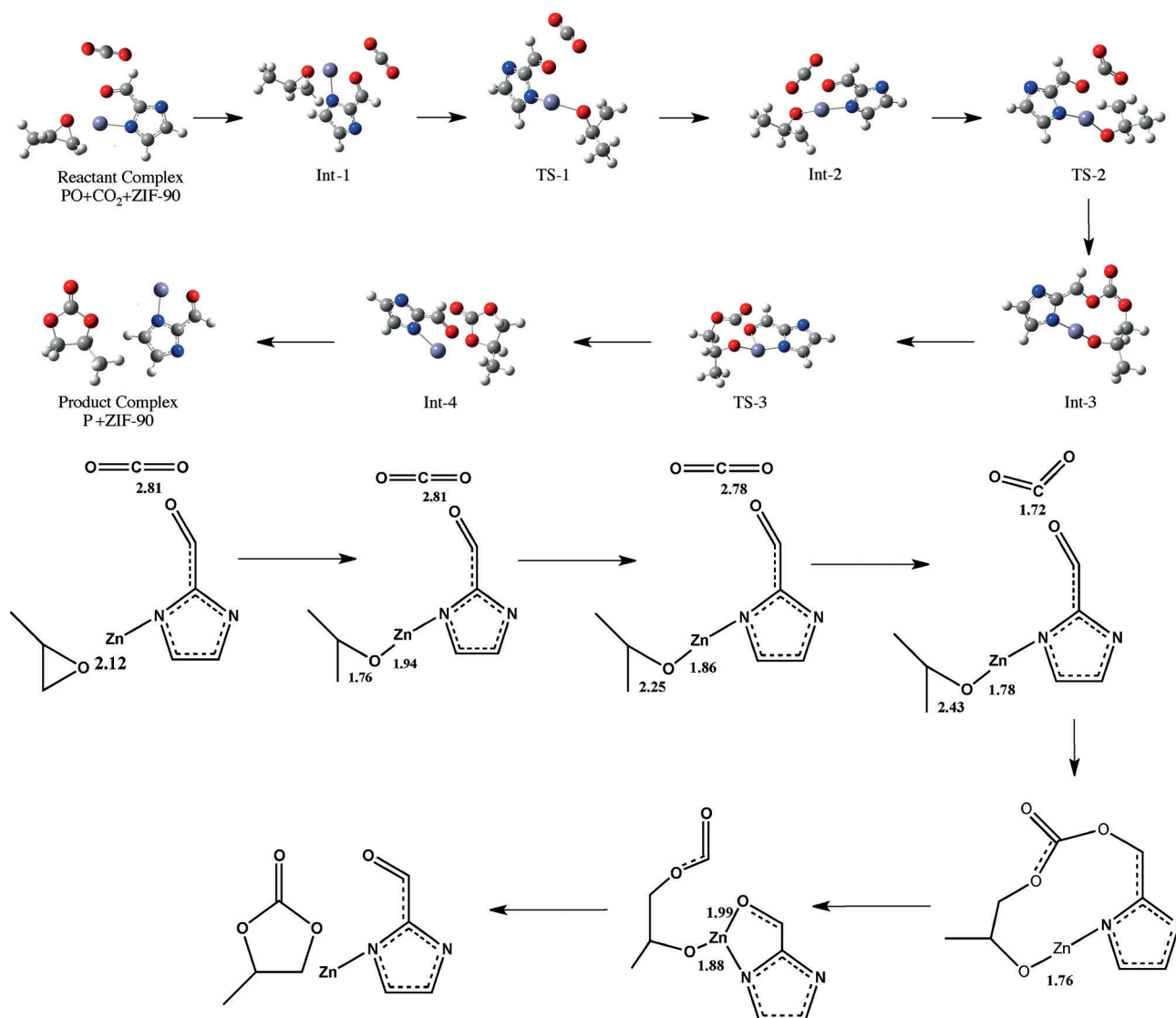
On the basis of the above DFT results and various previous studies, we put forth a plausible mechanism for the ZIF-90-catalyzed PO–CO<sub>2</sub> cycloaddition.<sup>[5,6,8]</sup> The TPD results clearly quantified the amount of acidic and basic sites in ZIF-90 (Table 1). In general, the zinc (Lewis acidic center) of ZIF-90 interacts with the oxygen atom of epoxide, which activates the epoxide ring. Meanwhile, the aldehyde group of ZIF-90 activates the CO<sub>2</sub>, whereby the ring-opened intermediate is formed,<sup>[9]</sup> which subsequently leads to the ring-closure step to produce PC (Scheme 2).

The reusability performance of ZIF-90 is illustrated in Figure 9. The spent catalyst was regenerated by centrifugation and washing with methanol. It was then filtered and dried at 60 °C for 24 hours. The regenerated catalyst was again used for the cycloaddition of PO and CO<sub>2</sub> under similar conditions. The results in Figure 9 show that the catalyst could be reused for at least five cycles without any considerable loss in its activity. The post-XRD analysis done after the first recycle of the reaction at 100 °C is shown in the Supporting Information (Figure S4).

### Conclusion

In conclusion, the catalytic ability of ZIF-90 toward PO–CO<sub>2</sub> cycloaddition was explored. ZIF-90, which is highly porous and contains imidazole-based ligands, produced a conversion of 88% under moderate reaction conditions of 120 °C and 1.2 MPa CO<sub>2</sub> for a duration of eight hours without any co-catalysts or solvents. The catalytic activity of ZIF-90 was compared to that of MOF-based catalysts reported to date for the cycloaddition of CO<sub>2</sub> and PO; ZIF-90 was an efficient catalyst in the absence of co-catalysts and solvents. On the basis of the DFT calculations, the role played by ZIF-90 in providing a favorable environment has been theoretically explained. A plausible mechanism in which ZIF-90 catalyzes the PO–CO<sub>2</sub> cycloaddition





**Scheme 2.** ZIF-90, CO<sub>2</sub>, and PO interactions from the DFT simulations. Int: Intermediate; TS: transition state; distances are in Å; atom color scheme is the same as in Figure 6.

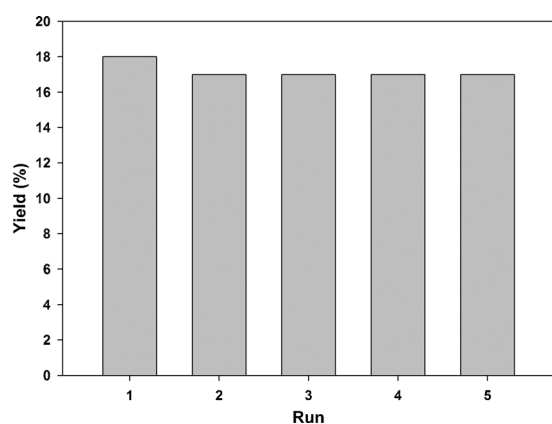


**Figure 9.** Recycle test. Reaction conditions: PO=42.8 mmol; time=8 h; temperature=100 °C; ZIF-90=30 mg;  $P_{\text{CO}_2}$ =1.2 MPa.

reaction has also been discussed on the basis of DFT calculations. The catalyst was able to undergo centrifuge separation and was recyclable for up to five cycles without any significant loss in catalytic activity.

### Acknowledgements

This study was supported by the National Research Foundation of Korea (GF-HIM 2013M3A6B1078877).

**Keywords:** cycloaddition • density functional calculations • metal–organic frameworks • propylene oxide • zeolites

- [1] A. Phan, C. J. Doonan, F. J. Uribe-Romo, C. B. Knobler, M. O’Keeffe, O. M. Yaghi, *Acc. Chem. Res.* **2010**, 43, 58.
- [2] a) R. Banerjee, A. Phan, B. Wang, C. Knobler, H. Furukawa, M. O’Keeffe, O. M. Yaghi, *Science* **2008**, 319, 939; b) J. C. Tan, T. D. Bennett, A. K. Cheetham, *Proc. Natl. Acad. Sci. USA* **2010**, 107, 9938; c) J. T. Hughes,

- T. D. Bennett, A. K. Cheetham, A. Navrotsky, *J. Am. Chem. Soc.* **2013**, *135*, 598; d) K. S. Park, Z. Ni, A. P. Cote, J. Y. Choi, R. Huang, F. J. Uribe-Romo, H. K. Chae, M. O'Keeffe, O. M. Yaghi, *Proc. Natl. Acad. Sci. USA* **2006**, *103*, 10186; e) S. K. Nune, P. K. Thallapally, A. Dohnalkova, C. Wang, J. Liu, G. J. Exarhos, *Chem. Commun.* **2010**, 46, 4878; f) O. Tziaila, Ch. Veziri, X. Papatryfon, K. G. Beltsios, A. Labropoulos, B. Iliev, G. Adamova, T. J. S. Schubert, M. C. Kroon, M. Francisco, L. F. Zubeir, G. E. Romanos, G. N. Karanikolos, *J. Phys. Chem. C* **2013**, *117*, 18434; g) D. W. Lewis, A. R. Ruiz-Salvador, A. Gomez, L. M. Rodriguez-Albelo, F. Coudert, B. Slater, A. K. Cheetham, C. Mellot-Draznieks, *CrystEngComm* **2009**, *11*, 2272.
- [3] a) K. Sumida, D. L. Rogow, J. A. Mason, T. M. McDonald, E. D. Bloch, Z. R. Herm, T. Bae, J. R. Long, *Chem. Rev.* **2012**, *112*, 724; b) S. Klaus, M. W. Lehenmeier, C. E. Anderson, B. Rieger, *Coord. Chem. Rev.* **2011**, *255*, 1460; c) A. J. Hunt, E. H. K. Sin, R. Marriott, J. H. Clark, *ChemSusChem* **2010**, *3*, 306; d) M. Mikkelsen, M. Jorgensen, F. C. Krebs, *Energy Environ. Sci.* **2010**, *3*, 43.
- [4] a) A. G. Shaikh, S. Sivaram, *Chem. Rev.* **1996**, *96*, 951; b) M. North, R. Pasquale, C. Young, *Green Chem.* **2010**, *12*, 1514; c) T. Sakakura, J. Choi, H. Yasuda, *Chem. Rev.* **2007**, *107*, 2365; d) D. J. Darensbourg, M. W. Holtcamp, *Coord. Chem. Rev.* **1996**, *153*, 155; e) H. Li, P. S. Bhadury, B. Song, S. Yang, *RSC Adv.* **2012**, *2*, 12525; f) N. Kihara, N. Hara, T. Endo, *J. Org. Chem.* **1993**, *58*, 6198.
- [5] a) T. Yano, H. Matsui, T. Koike, H. Ishiguro, H. Fujihara, M. Yoshihara, T. Maeshima, *Chem. Commun.* **1997**, 1129; b) B. M. Bhanage, S. I. Fujita, Y. Ikushima, M. Arai, *Appl. Catal. A* **2001**, *219*, 259; c) H. Yasuda, L. N. He, T. Sakakura, *J. Catal.* **2002**, *209*, 547; d) M. Tu, R. J. Davis, *J. Catal.* **2001**, *199*, 85; e) H. Kawanami, Y. Ikushima, *Chem. Commun.* **2000**, 2089; f) R. Srivastava, D. Srinivas, P. Ratnasamy, *Catal. Lett.* **2003**, *91*, 133; g) H. Xie, S. Li, S. Zhang, *J. Mol. Catal. A: Chem.* **2006**, *250*, 30; h) J. Tharun, M. M. Dharman, Y. Hwang, R. Roshan, M. S. Park, D. W. Park, *Appl. Catal. A* **2012**, *419–420*, 178; i) J. Tharun, Y. Hwang, R. Roshan, S. Ahn, A. C. Kathalikkattil, D. W. Park, *Catal. Sci. Technol.* **2012**, *2*, 1674; j) J. Tharun, D. W. Kim, R. Roshan, Y. Hwang, D. W. Park, *Catal. Commun.* **2013**, *31*, 62; k) K. R. Roshan, G. Mathai, J. Kim, J. Tharun, G. A. Park, D. W. Park, *Green Chem.* **2012**, *14*, 2933; l) J. Tharun, G. Mathai, R. Roshan, A. C. Kathalikkattil, K. Bomi, D. W. Park, *Phys. Chem. Chem. Phys.* **2013**, *15*, 9029; m) K. R. Roshan, T. Jose, A. C. Kathalikkattil, D. W. Kim, B. Kim, D. W. Park, *Appl. Catal. A* **2013**, *467*, 17; n) K. R. Roshan, T. Jose, D. Kim, K. A. Cherian, D. W. Park, *Catal. Sci. Technol.* **2014**, *4*, 963; o) D. W. Kim, R. Roshan, J. Tharun, A. Cherian, D. W. Park, *Korean J. Chem. Eng.* **2013**, *30*, 1973; p) J. Sun, W. Cheng, Z. Yang, J. Wang, T. Xu, J. Xin, S. Zhang, *Green Chem.* **2014**, *16*, 3071.
- [6] a) M. Zhu, M. A. Carreon, *J. Appl. Polym. Sci.* **2014**, *131*, 39738; b) A. C. Kathalikkattil, D. W. Kim, J. Tharun, H. G. Soek, R. Roshan, D. W. Park, *Green Chem.* **2014**, *16*, 1607; c) A. C. Kathalikkattil, D. W. Park, *J. Nanosci. Nanotechnol.* **2013**, *13*, 2230; d) Y. J. Kim, D. W. Park, *J. Nanosci. Nanotechnol.* **2013**, *13*, 2307; e) M. Zhu, D. Srinivas, S. Bhogeswararao, P. Ratnasamy, M. A. Carreon, *Catal. Commun.* **2013**, *32*, 36; f) O. V. Zalomaeva, A. M. Chibiryayev, K. A. Kovalenko, O. A. Kholdeeva, B. S. Balzhinimaev, V. P. Fedin, *J. Catal.* **2013**, *298*, 179; g) C. M. Miralda, E. E. Macias, M. Zhu, P. Ratnasamy, M. A. Carreon, *ACS Catal.* **2012**, *2*, 180; h) O. V. Zalomaeva, N. V. Maksimchuk, A. M. Chibiryayev, K. A. Kovalenko, V. P. Fedin, B. S. Balzhinimaev, *J. Energy Chem.* **2013**, *22*, 130; i) M. A. Carreon, *Indian J. Chem.* **2012**, *51A*, 1306; j) T. Lescouet, C. Chizallet, D. Farrusseng, *ChemCatChem* **2012**, *4*, 1725; k) E. E. Macias, P. Ratnasamy, M. A. Carreon, *Catal. Today* **2012**, *198*, 215; l) H. Y. Cho, D. A. Yang, J. Kim, S. Y. Jeong, W. S. Ahn, *Catal. Today* **2012**, *185*, 35; m) X. Zhou, Y. Zhang, X. Yang, L. Zhao, G. Wang, *J. Mol. Catal. A: Chem.* **2012**, *361–362*, 12; n) A. C. Kathalikkattil, R. Roshan, J. Tharun, H. G. Soek, H. S. Ryu, D. W. Park, *ChemCatChem* **2014**, *6*, 284; o) W. Kleist, F. Jutz, M. Maciejewski, A. Baiker, *Eur. J. Inorg. Chem.* **2009**, 3552; p) Y. Ren, Y. Shi, J. Chen, S. Yang, C. Qi, H. Jiang, *RSC Adv.* **2013**, *3*, 2167; q) Y. Ren, X. Cheng, S. Yang, C. Qi, H. Jiang, Q. Mao, *Dalton Trans.* **2013**, 42, 9930; r) D. A. Yang, H. Y. Cho, J. Kim, S. T. Yang, W. S. Ahn, *Energy Environ. Sci.* **2012**, *5*, 6465; s) J. Kim, S. N. Kim, H. G. Jang, G. Seo, W. S. Ahn, *Appl. Catal. A* **2013**, *453*, 175; t) J. Song, Z. Zhang, S. Hu, T. Wu, T. Jiang, B. Han, *Green Chem.* **2009**, *11*, 1031.
- [7] a) S. Liu, Z. Xiang, Z. Hu, X. Zheng, D. Cao, *J. Mater. Chem.* **2011**, *21*, 6649; b) C. Y. Sun, C. Qin, X. L. Wang, G. S. Yang, K. Z. Shao, Y. Q. Lan, Z. M. Su, P. Huang, C. G. Wang, E. B. Wang, *Dalton Trans.* **2012**, 41, 6906; c) O. Karagiari, M. B. Lalonde, W. Bury, A. A. Sarjeant, O. K. Farha, J. T. Hupp, *J. Am. Chem. Soc.* **2012**, *134*, 18790; d) A. Huang, J. Caro, *Angew. Chem. Int. Ed.* **2011**, *50*, 4979; *Angew. Chem.* **2011**, *123*, 5083; e) A. Huang, N. Wang, C. Kong, J. Caro, *Angew. Chem. Int. Ed.* **2012**, *51*, 10551; *Angew. Chem.* **2012**, *124*, 10703; f) A. U. Ortiz, A. P. Freitas, A. Boutin, A. H. Fuchs, F. X. Coudert, *Phys. Chem. Chem. Phys.* **2014**, *16*, 9940; g) J. A. Gee, J. Chung, S. Nair, D. S. Sholl, *J. Phys. Chem. C* **2013**, *117*, 3169; h) W. Morris, C. J. Doonan, H. Furukawa, R. Banerjee, O. M. Yaghi, *J. Am. Chem. Soc.* **2008**, *130*, 12626.
- [8] L. Yang, L. Yu, G. Diao, M. Sun, G. Cheng, S. Chen, *J. Mol. Catal. A: Chem.* **2014**, *392*, 278.
- [9] H. Amrouche, S. Aguado, J. P. Pellitero, C. Chizallet, F. Siperstein, D. Farrusseng, N. Bats, C. N. Draghi, *J. Phys. Chem. C* **2011**, *115*, 16425.
- [10] Gaussian 09, Revision B.01, M. J. Frisch, G. W. Trucks, H. B. Schlegel, G. E. Scuseria, M. A. Robb, J. R. Cheeseman, G. Scalmani, V. Barone, B. Menucci, G. A. Petersson, H. Nakatsuji, M. Caricato, X. Li, H. P. Hratchian, A. F. Izmaylov, J. Bloino, G. Zheng, J. L. Sonnenberg, M. Hada, M. Ehara, K. Toyota, R. Fukuda, J. Hasegawa, M. Ishida, T. Nakajima, Y. Honda, O. Kitao, H. Nakai, T. Vreven, J. A. Montgomery, Jr., J. E. Peralta, F. Ogliaro, M. Bearpark, J. J. Heyd, E. Brothers, K. N. Kudin, V. N. Staroverov, T. Keith, R. Kobayashi, J. Normand, K. Raghavachari, A. Rendell, J. C. Burant, S. S. Iyengar, J. Tomasi, M. Cossi, N. Rega, J. M. Millam, M. Klene, J. E. Knox, J. B. Cross, V. Bakken, C. Adamo, J. Jaramillo, R. Gomperts, R. E. Stratmann, O. Yazyev, A. J. Austin, R. Cammi, C. Pomelli, J. W. Ochterski, R. L. Martin, K. Morokuma, V. G. Zakrzewski, G. A. Voth, P. Salvador, J. J. Dannenberg, S. Dapprich, A. D. Daniels, O. Farkas, J. B. Foresman, J. V. Ortiz, J. Cioslowski, D. J. Fox, Gaussian, Inc., Wallingford CT, **2010**.

Received: November 15, 2014

Published online on ■■■■■, 0000

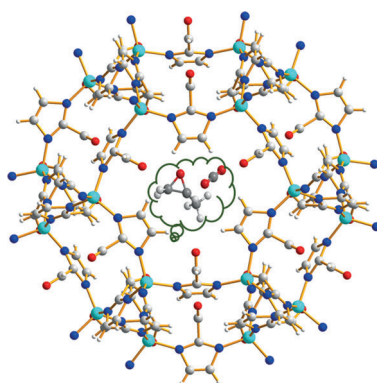
## FULL PAPERS

J. Tharun, G. Mathai, A. C. Kathalikkattil,  
R. Roshan, Y.-S. Won, S. J. Cho,  
J.-S. Chang, D.-W. Park\*

■■■ – ■■■



**Exploring the Catalytic Potential of  
ZIF-90: Solventless and Co-Catalyst-  
Free Synthesis of Propylene  
Carbonate from Propylene Oxide and  
CO<sub>2</sub>**



**The cage is a gateway:** ZIF-90, a highly porous zeolitic imidazolate framework with a colossal cage (see figure), acts as a catalytic gateway to the propylene oxide (PO)–CO<sub>2</sub> cycloaddition reaction without any co-catalysts or solvents under moderate reaction conditions. DFT calculations were performed to understand the role played by ZIF-90 in creating a favorable environment for the PO–CO<sub>2</sub> cycloaddition reaction.